Constructi*ng* 1D/2D Interwoven Carbonous Matrix *to Enable* High-Efficiency Sulfur Immobilization in Li-S Battery

Jiafeng Ruan[1,2#], Hao Sun[1#], Yun Song[2], Yuepeng Pang[1], Junhe Yang[1], Shiyou Zheng[1,]*

[1]School of Materials and Chemistry, University of Shanghai for Science and Technology, Shanghai 200093, People's Republic of China.

[2]Department of Materials Science, Fudan University, Shanghai 200433, People's Republic of China.

[*]Corresponding Author: syzheng@usst.edu.cn

Experimental Section

Synthesis of SG-CNT: The SG-CNT is synthesized from Multi-wall CNT by a modified Hummer's method (the purity of CNT is >95%, the diameter of the CNT is around 11 nm, the average length is around 10 μm, CNano Technology Ltd.). Before transferring the oxidized CNT to the hydrothermal reactor, the solution (the solution concentration is around 10 mg mL^{-1}) is ultrasonicated for half hour. After that, the solution of the O-CNT is placed into Teflon-lined stainless-steel autoclave for hydrothermal at 200 °C for 48 h. Finally, the as-prepared SG-CNT hydrogel is freeze-dried.

Synthesis of S@SG-CNT composite: The S@SG-CNT composite is prepared by infiltration of the sublimed S powder (Sigma-Aladdin) into SG-CNT in evacuated quartz capsule (mass ratios of $m_{SG\text{-}CNT}$: m_S=3:7) at 700 ºC for 6 h. First of all, the SG-CNT and S powder are added in the quartz capsule. After that, through the vacuum of the quartz capsule to ensure S infiltrate into the SG-CNT completely at 700 ºC. And then, we can easily obtain the S@SG-CNT composite after cooling down to room temperature. For comparisons, the S@CNT and S@O-CNT composite are prepared by carbonizing of merging the pure CNT and O-CNT with sublimed S, respectively.

Physical characterizations: SEM images are obtained by using a FEI Nova SEM 230 equipped with HR-SEM (form Oxford Instruments, named INCA X-Max 80). Deeply morphologies and microstructure are characterized by performed a TEM at 200 kV (JEOL Ltd. from Japan), which named JEM-2100F. The XRD patterns are recorded on the X-ray diffractometer (Rigaku D/MAX-2200/PC) with a Cu Kα radiation at 40 kV and 20 mA. Raman spectra is obtained by a Senterra R200-L (from Germany). The surface properties are analyzed by XPS (Kratos Axis Ultra DLD). BET surface areas and porosity for the as-synthesized sample is carried out by using a N_2 sorption instrument (Micromeritics, ASAP2020). To confirmed the S content in the S@CNT, S@O-CNT and S@SG-CNT composites, thermogravimetric analysis (TGA) is performed with a heating rate of 10 ^oC/min (a Netzsch STA 449 F1, Germany), and high-purity N_2 as the purge gas.

Electrochemical measurements: The electrochemical performance of the Li-S battery is performed using 2032 half-cell. The SG-CNT matrix is mixed with carbon black and polyvinylidene fluoride (PVDF) in a weight ratio of 85:5:10, with N-methylpyrrolidone (NMP) solvent as a dispersant. After stirring 2h, the as-prepared slurry is coated onto an Al foil. After that, the electrodes are punched into circle discs, and the diameter and loading of the electrodes is 1.2 cm and ~2.4 mg cm^{-2}, respectively. Besides, the three kinds of high mass loading are 4.1, 5.3, and 6.6 mg cm^{-2}. The battery assembly is performed in the glovebox (MBRAUN). Before being transferred to the glovebox, the composite electrodes should further dry in a vacuum at 60 °C over for 24 h. Li metal is used as a counter; Celgard 3501 (Celgard, LLC Corp., USA) is used as a separator; 1.0 M LiTFSI dissolved in a mixture of 1,3 DOL/1,2 DME (1:1 v/v) with 1.0 % wt. $LiNO_3$ additive is used as the electrolyte. The electrolyte/S ratios are 11 μL mg^{-1} and 8 μL mg^{-1} for cathodes with S loading of ~2.4 mg cm^{-2} and higher S loading (4.1 mg cm^{-2}; 5.3 mg cm^{-2}; 6.6 mg cm^{-2}), respectively. Cycling performances are conducted at various rates in the potential range of 1.5 to 3.0 V (vs Li/Li^+) on LAND CT2001A battery test system (Wuhan Jinnuo Electronics, Ltd.). CV tests are

performed at a scan rate of 0.1 mV s^{-1} (Gamry Co., Reference 3000, USA). EIS is measured at room temperature (~25 °C). The frequency ranged from 0.1 Hz to 100 kHz. Before any EIS tests, the cell should be cycle to the target cycle number at 2.0 A g^{-1}. Li_2S_6 adsorption test: 0.02 M Li_2S_6 dissolve in DOL/DME with a volumetric ratio of 1/1. The three matrixes are added 15 mg in the above solution.

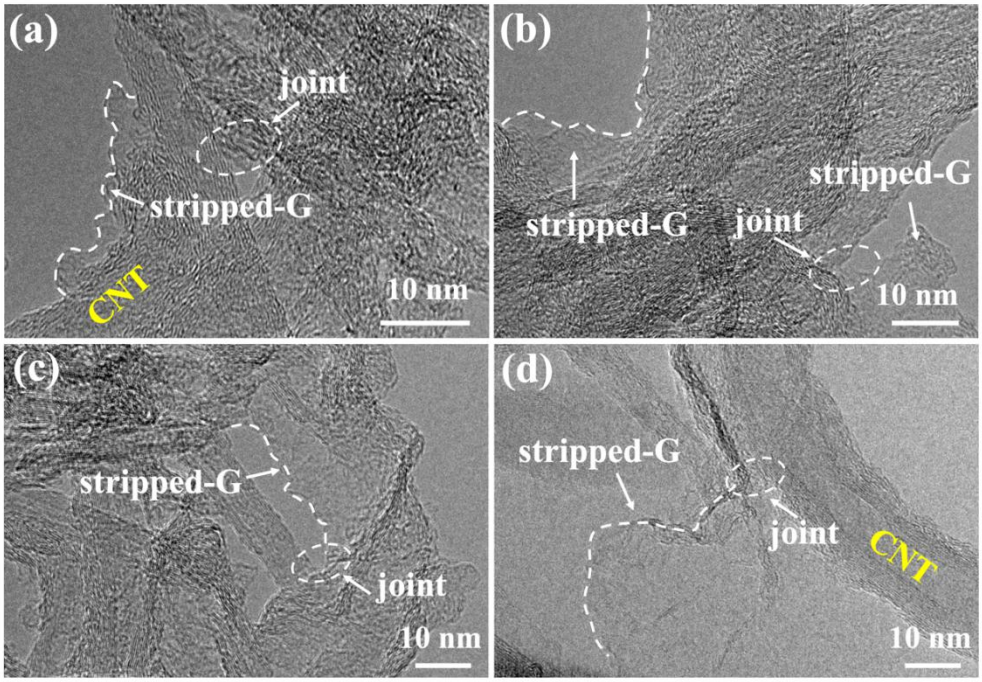

Figure S1. TEM images of the (a) SG-CNT-6; (b) SG-CNT-12; (c) SG-CNT-24; (d) SG-CNT.

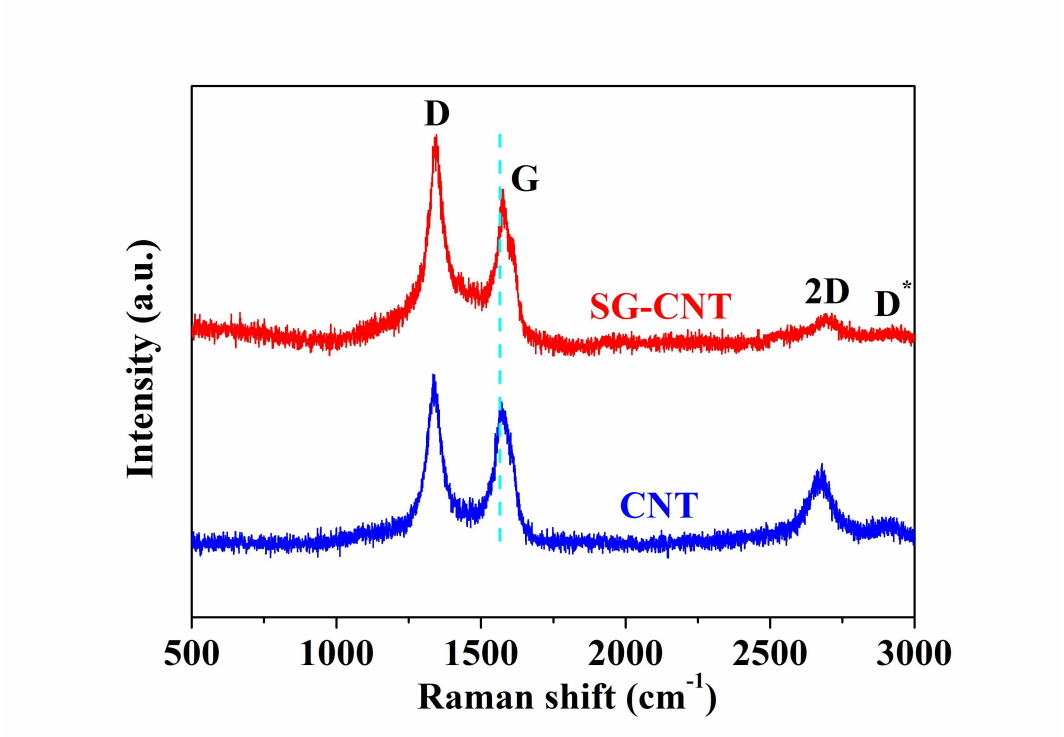

Figure R2. Raman patterns of CNT and SG-CNT

The 2D peak originates from a two-phonon and second-order scattering process and its intensity is especially sensitive to the sample purity and long-range order. A weak D* band affiliated to the G band is also indicative of carbon disorder degree. The remarkably decreased I_{2D}/I_G and up-shifted G band (due to the emerged D* band) suggest that the intact tube walls have been gradually unraveled in the consecutive unzipping process, resulting in the formation of graphene.

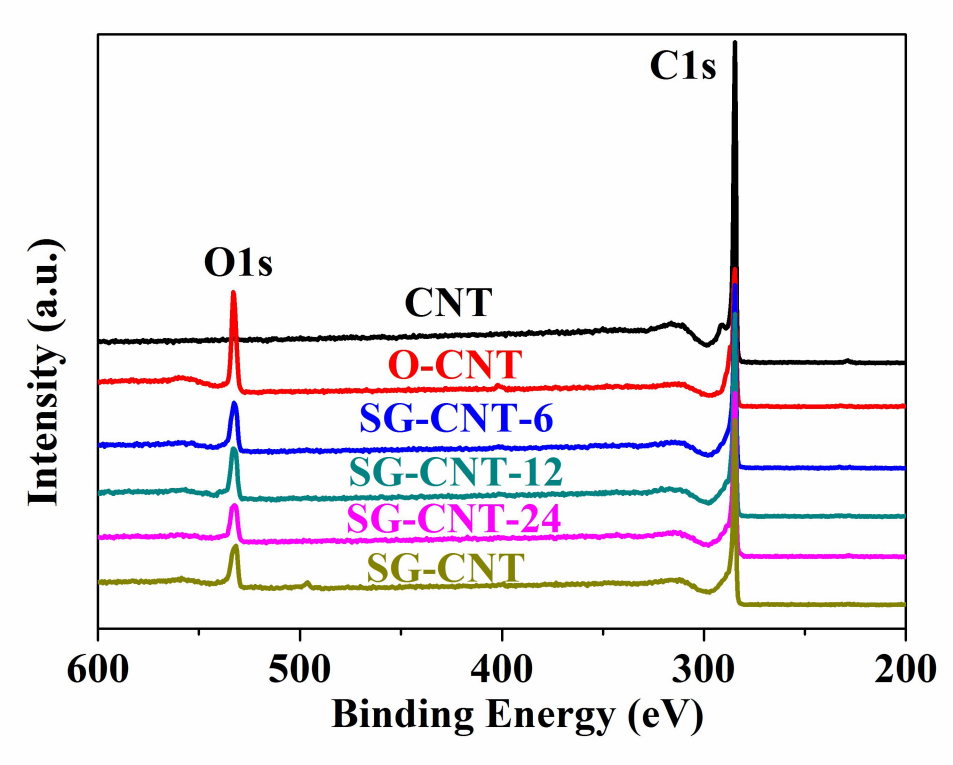

Figure S3. XPS survey of CNT, O-CNT, SG-CNT-6, SG-CNT-12, SG-CNT-24 and SG-CNT.

Table S1. Elemental composition of the CNT, O-CNT, SG-CNT-6, SG-CNT-12, SG-CNT-24 and SG-CNT.

Sample	at. % C	at. % O	O/C
CNT	99.66	0.34	0.003
O-CNT	77.61	22.39	0.288
SG-CNT-6	85.85	14.15	0.165
SG-CNT-12	86.01	13.99	0.163
SG-CNT-24	86.13	13.87	0.161
SG-CNT	86.65	13.35	0.154

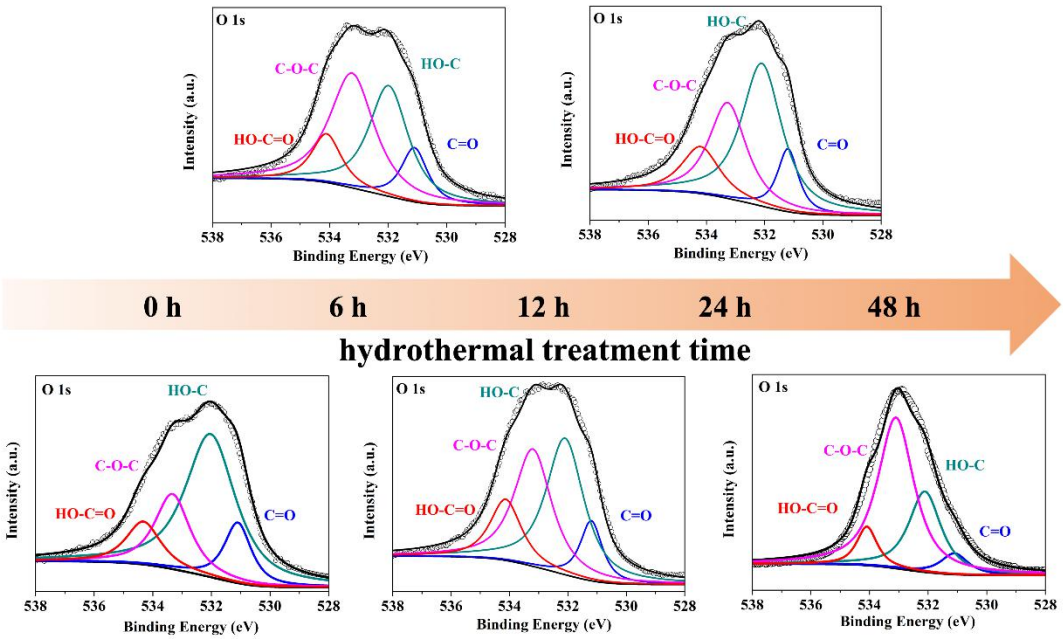

Figure S4. The high-resolution XPS spectrum of O 1s.

Table S2. Assignments and percentage composition in the O 1s regions of the CNT, O-CNT and SG-CNT.

	functional group	binding energy (eV)	actual ratios (% area)		
			O-CNT	SG-CNT-12	SG-CNT
O 1s	C=O	531.2	2.83	1.45	0.8
	HO-C	532.0	12.47	5.65	3.69
	C-O-C	533.2	4.53	4.80	7.73
	HO-C=O	534.3	2.55	2.09	1.12

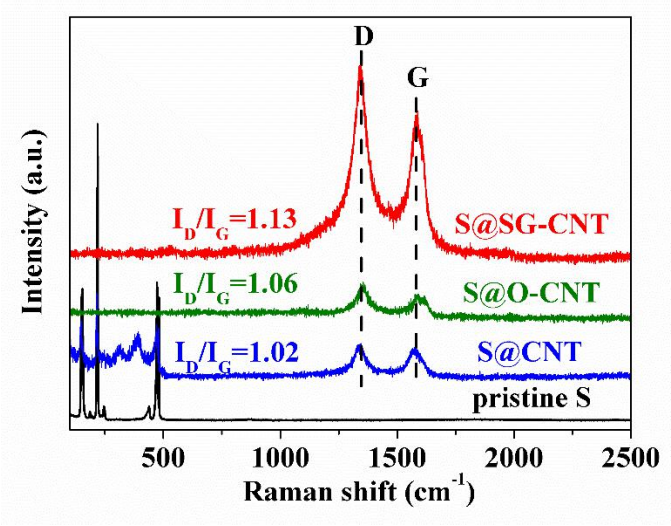

Figure S5. Raman patterns of pristine S, S@CNT, S@O-CNT and S@SG-CNT

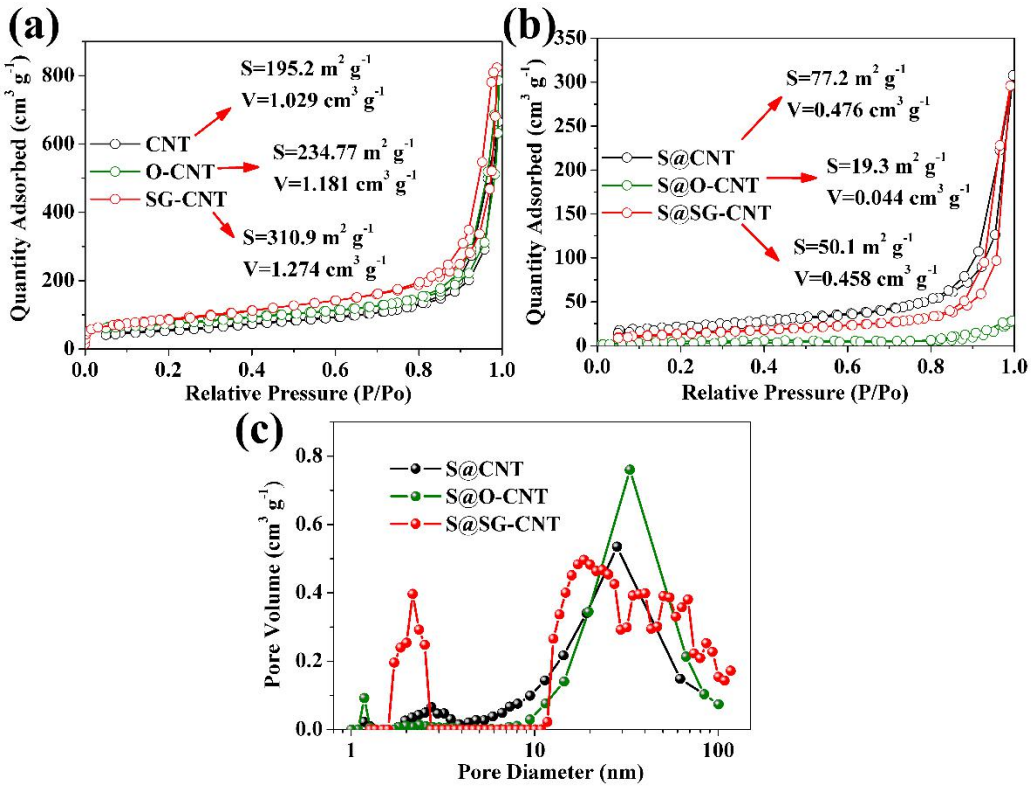

Figure S6. (a) N2 adsorption isotherms of CNT, O-CNT and SG-CNT; (b) N2 adsorption isotherms of S@CNT, S@O-CNT and S@SG-CNT; (c) pore size distribution of S@CNT, S@O-CNT and S@SG-CNT.

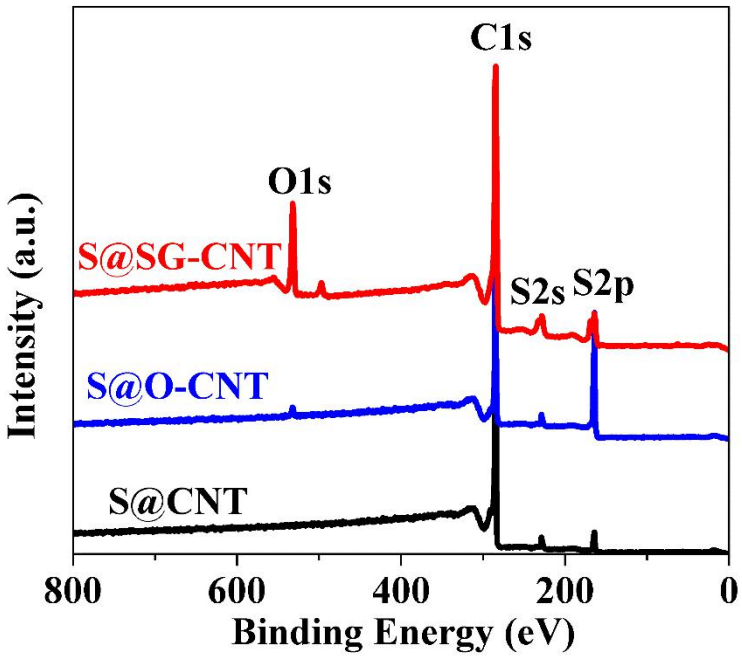

Figure S7. XPS survey of the S@CNT, S@O-CNT and S@SG-CNT

Table S3. Elemental composition of S@CNT, S@O-CNT and S@SG-CNT composites.

	at. % C	at. % O	at. % S	O/C
S@CNT	86.37	0.18	13.45	0.002
S@O-CNT	81.91	1.97	16.12	0.024
S@SG-CNT	72.93	11.58	15.49	0.159

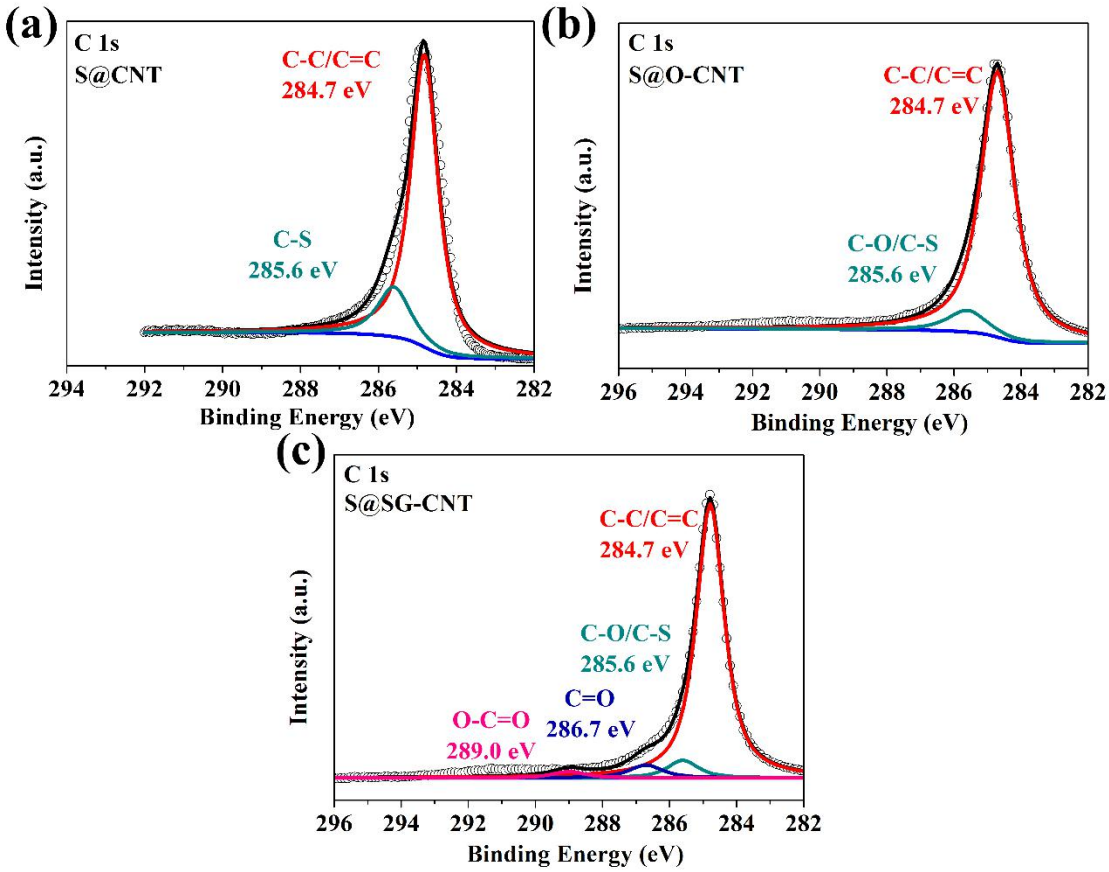

Figure S8. The high-resolution XPS spectrum of C 1s.

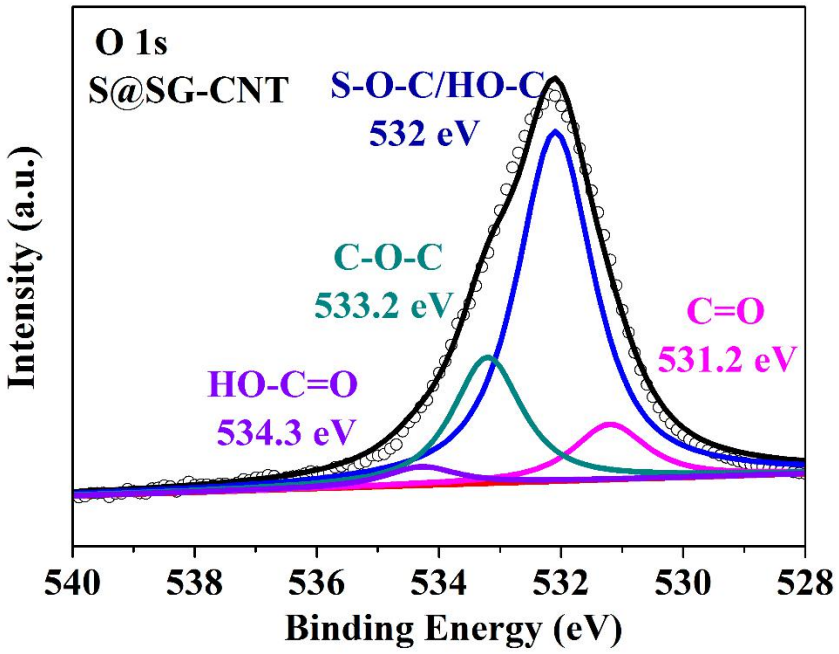

Figure S9. The high-resolution XPS spectrum of O 1s.

Table S4. Assignments and percentage composition in the C1s, O 1s, and S 2p regions of the S@CNT, S@O-CNT and S@SG-CNT composites.

	functional group	binding energy (eV)	ratios (% area)		
			S@CNT	S@O-CNT	S@SG-CNT
C 1s	C-C/C=C	284.7	83.2	74.1	67.9
	C-S	285.6	16.8	13.9	13.1
	C=O	286.7	-	-	7.1
	O-C=O	289.0	-	-	11.9
O 1s	C=O	531.2	-	-	9.8
	S-O-C/HO-C	532	-	-	65.6
	C-O-C	533.2	-	-	21.3
	HO-C=O	534.3	-	-	3.3
S 2p	S-S/S-C	163.9	74.6	67.2	36.9
	S-S/S-C	165.1	25.4	28.8	20.3
	S-O	168.7	-	2.2	23.1
	S-O	170.0	-	1.8	19.7

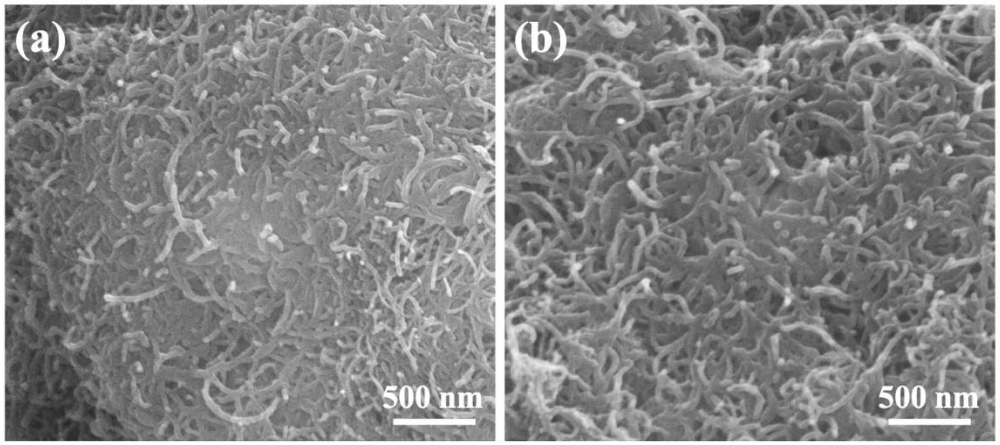

Figure S10. SEM images of the (a) S@CNT and (b) S@O-CNT

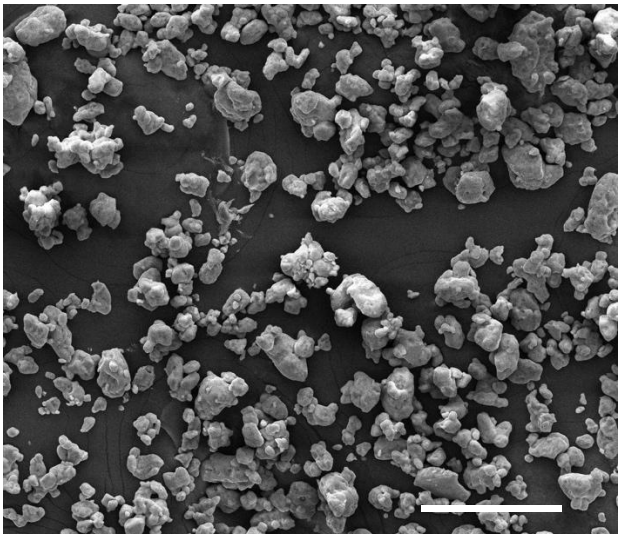

Figure S11. SEM image of the pure S. This scale bar is 100 μm.

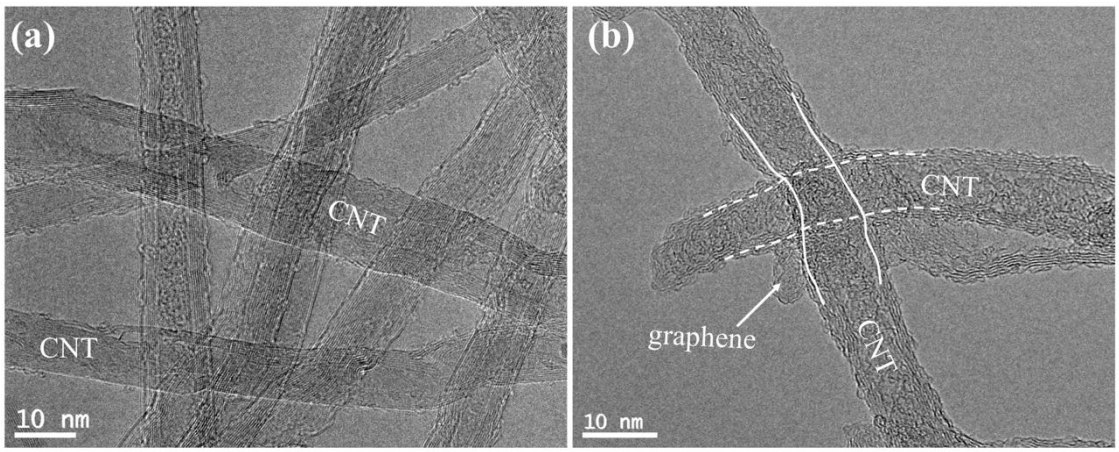

Figure S12. TEM images of the (a) S@CNT and (b) S@O-CNT.

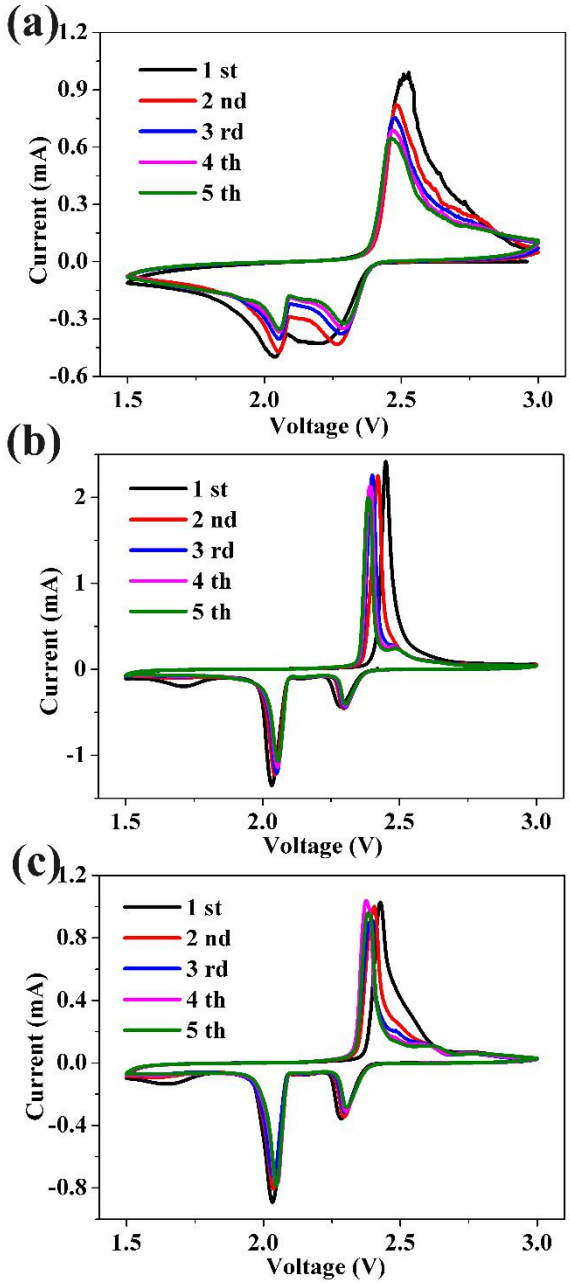

Figure S13. Cyclic voltammetry curves of the (a) pure S, (b) S@S-CNT, and (c) S@O-CNT electrode at a scan rate of 0.1 mV s^{-1}.

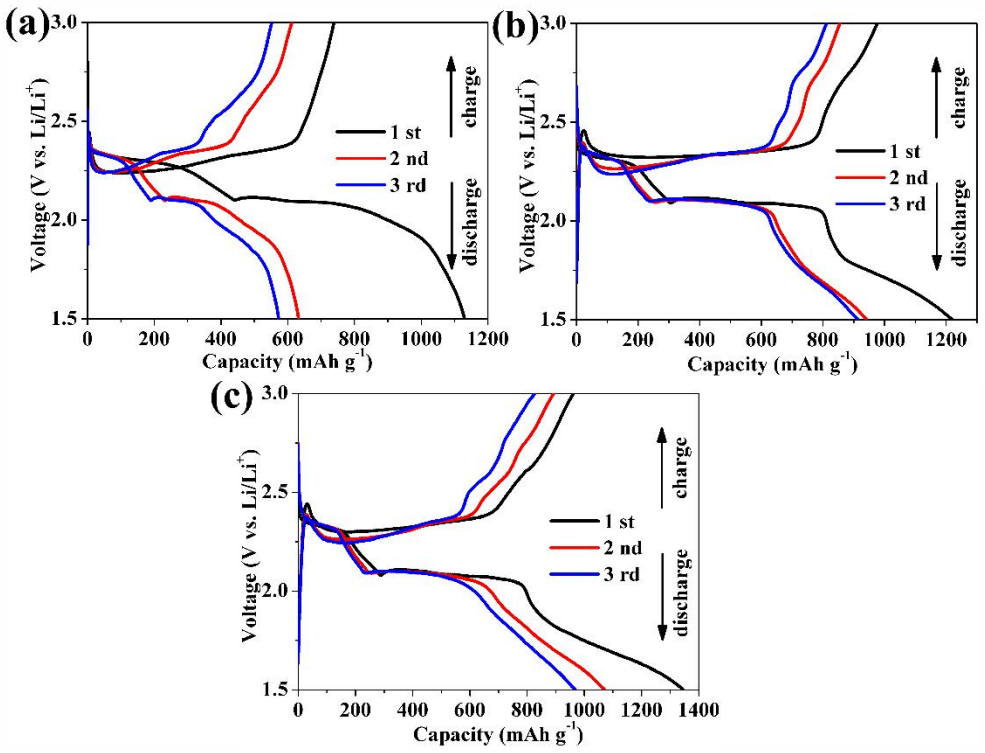

Figure S14. Initial three discharge/charge profiles of the pure S, S@CNT and S@O-CNT electrodes at a current density of 0.1 A g^{-1}.

Table S5. Re and **Rct** obtained by fitting experimental data in Figure S13 using equivalent circuit (inset in Figure S13) for S@SG-CNT cell before and after cycling.

	Fresh cell	After 3 cycles	After 300 cycles	After 500 cycles	After 1000 cycles
Re (Ω)	6.9	5.9	7.2	6.1	5.1
Rct (Ω)	132	34.1	50.4	55.8	57.7

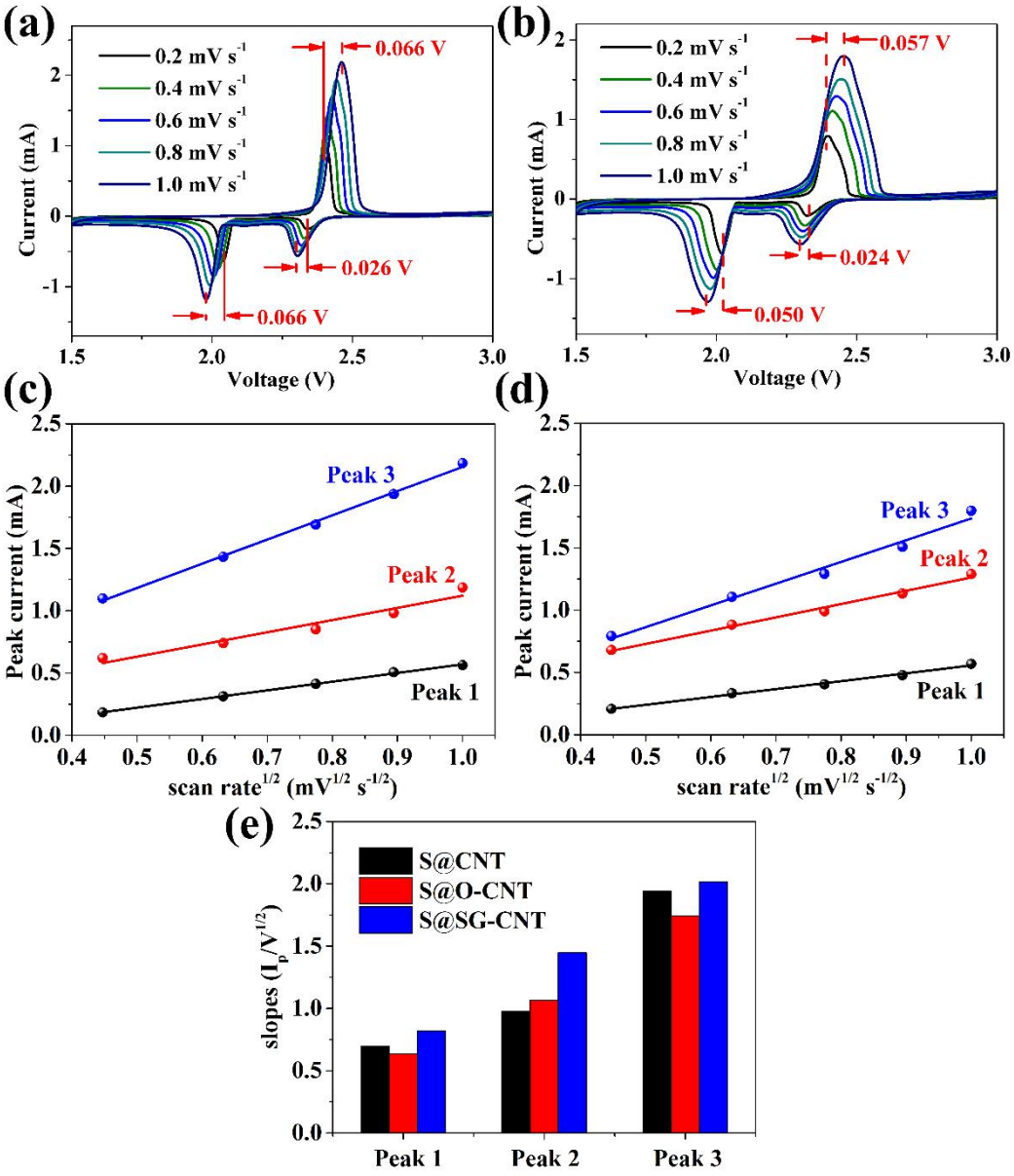

Figure S15. the cyclic voltammograms of the (a) S@CNT and (b) S@O-CNT at various scan rates; linear fits of the peak current of the (c) S@CNT and (d) S@O-CNT composites for different peaks; (e) the corresponding slope value of $I_p/V^{1/2}$.

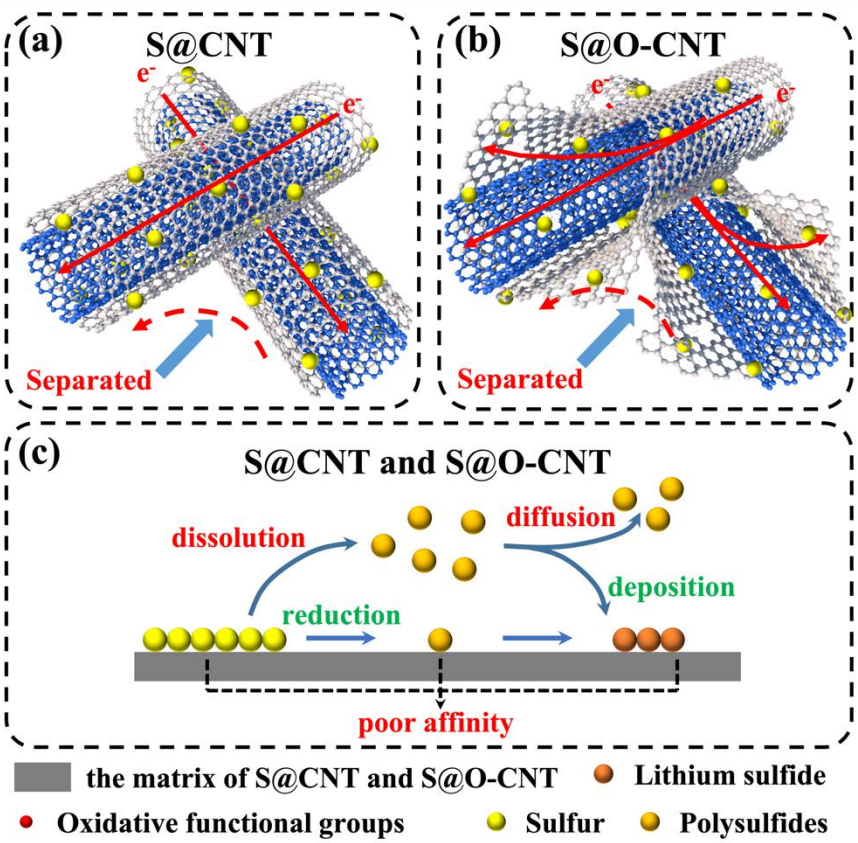

Figure S16. Schematic illustration of the electrochemical reaction mechanism of the S@CNT and S@O-CNT.